



Short communication

A novel cobalt-free layered perovskite-type $\text{GdBaFeNiO}_{5+\delta}$ cathode material for proton-conducting intermediate temperature solid oxide fuel cells

Zhijie Yang, Zuolong Ding, Jia Xiao, Hongmin Zhang, Guilin Ma*, Zhufa Zhou**

Key Laboratory of Organic Synthesis of Jiangsu Province, College of Chemistry, Chemical Engineering and Materials Science, Soochow University, Suzhou 215123, China

HIGHLIGHTS

- ▶ A novel cobalt-free cathode material $\text{GdBaFeNiO}_{5+\delta}$ for IT-SOFC was prepared.
- ▶ The conductivity of $\text{GdBaFeNiO}_{5+\delta}$ reached 185 S cm^{-1} in oxygen at 375°C .
- ▶ An anode-supported BZCY electrolyte membrane was prepared by a simple process.
- ▶ Peak power density of the cell H_2 , Ni-BZCY|BZCY|GBFN, air was 456 mW cm^{-2} at 700°C .

ARTICLE INFO

Article history:

Received 25 April 2012

Received in revised form

13 July 2012

Accepted 16 July 2012

Available online 1 August 2012

Keywords:

Layered perovskite

Cathode

Conductivity

Solid oxide fuel cell

ABSTRACT

The $\text{GdBaFeNiO}_{5+\delta}$ (GBFN) oxide is prepared by the citric-nitrate process and investigated as a novel cathode material for proton-conducting intermediate temperature solid oxide fuel cells (IT-SOFCs). The conductivities of GBFN reach a maximum of 112 S cm^{-1} under argon, 161 S cm^{-1} under air and 185 S cm^{-1} under oxygen at 375°C . An anode-supported $\text{BaZr}_{0.1}\text{Ce}_{0.7}\text{Y}_{0.2}\text{O}_{3-\alpha}$ (BZCY) electrolyte membrane is successfully fabricated by a simple, cost-effective spin coating process. Peak power densities of the hydrogen/air fuel cell using BZCY electrolyte membrane and GBFN cathode reach 171 mW cm^{-2} at 600°C , 280 mW cm^{-2} at 650°C and 456 mW cm^{-2} at 700°C , respectively. The interfacial polarization resistance (R_p) for the fuel cell is as low as $0.15 \Omega \text{ cm}^2$ at 700°C under open circuit conditions.

© 2012 Elsevier B.V. All rights reserved.

1. Introduction

Fuel cell as a new power-generation device has attracted worldwide attention since it may be of greater benefit over traditional energy conversion systems including high power conversion efficiency, fuel adaptability, reliability, little environment pollution and so on [1–3]. Among fuel cells, intermediate-temperature solid oxide fuel cell (IT-SOFC) has excited the especial interest of all. This is because it has many advantages of both low and high-temperature fuel cell [4,5]: (1) fast electrode reaction rate; (2) high tolerance performance for CO and other impurities; (3) favorable selectivity for sealing materials and connection materials; (4) easy management in water and thermal cycles, etc.

A typical SOFC essentially consists of porous anode and cathode as well as dense ion conducting electrolyte. Compared to YSZ as an oxide-ionic conducting electrolyte, BaCeO_3 -based proton conducting electrolyte exhibits lower activation energy and higher ionic conductivity as well as energy efficiency at intermediate temperatures of $300\text{--}800^\circ\text{C}$. However, doped BaCeO_3 displays poor chemical stability in water vapor and carbon dioxide containing atmospheres. In contrast, doped BaZrO_3 displays sufficiently high chemical stability in spite of lower conductivity [6]. Recently, a new composite oxide based on BaZrO_3 and BaCeO_3 , $\text{BaZr}_{0.1}\text{Ce}_{0.7}\text{Y}_{0.2}\text{O}_{3-\delta}$ (BZCY), has been extensively utilized as proton conducting electrolyte material for IT-SOFCs due to its both high ionic conductivity and sufficient chemical stability under the conditions relevant to fuel cell operations [7].

However, the polarization resistance of cathode–electrolyte interface rapidly increases as temperature decreases from high temperature to intermediate temperature [8]. Accordingly, there is much interest in developing suitable cathode materials for IT-SOFCs. Many cathode materials with simple perovskite structure,

* Corresponding author. College of Chemistry, Chemical Engineering and Materials Science, Dushu Lake Campus of Soochow University, Suzhou 215123, China. Tel.: +86 512 65880326; fax: +86 512 65880089.

** Corresponding author. Tel.: +86 512 65880326; fax: +86 512 65880089.

E-mail address: 32uumagl@suda.edu.cn (G. Ma).

such as $\text{Ba}_{0.5}\text{Sr}_{0.5}\text{Co}_{0.8}\text{Fe}_{0.2}\text{O}_{3-\delta}$ (BSCF) [2], $\text{Ba}_{0.5}\text{Sr}_{0.5}\text{Fe}_{0.9}\text{Mo}_{0.1}\text{O}_{3-\delta}$ (BSFM) [9] and $\text{Ba}_{0.6}\text{Sr}_{0.4}\text{Co}_{0.9}\text{Nb}_{0.1}\text{O}_{3-\delta}$ (BSCN) [10], have been extensively reported due to the low polarization resistance and the high oxygen reduction activation for IT-SOFCs. Recently, the cathode materials with layered perovskite structure for IT-SOFCs, such as $\text{GdBaCo}_2\text{O}_{5+\delta}$ (GBC) [11], $\text{GdBaCo}_{2/3}\text{Fe}_{2/3}\text{Cu}_{2/3}\text{O}_{5+\delta}$ (GBCFC) [12], $\text{SmBaCo}_2\text{O}_{5+\delta}$ (SBC) [13] and $\text{NdBaCo}_2\text{O}_{5+\delta}$ (NBC) [14], have attracted considerable attention. This is because the oxygen-ion diffusion in the layered perovskite structure may be enhanced by several orders of magnitude, resulting from alternant ordering of lanthanide and alkali-earth ion layers and the oxygen vacancies mainly located in the rare earth layers in the A-sites [15,16].

In this paper, a novel cobalt-free cathode material $\text{GdBaFeNiO}_{5+\delta}$ (GBFN) with a layered perovskite structure for IT-SOFCs was prepared by a citric-nitrate process. The electrical conduction in GBFN was investigated under various atmospheres. The fuel cell with GBFN cathode and proton conducting BZCY electrolyte was assembled and tested from 600 to 700 °C with hydrogen as the fuel and air as the oxidant.

2. Experimental

2.1. Preparation of GBFN and BZCY powders

The $\text{GdBaFeNiO}_{5+\delta}$ (GBFN) powders used as cathode materials for IT-SOFC were prepared by a citric-nitrate process. All the reagents used were analytical-grade (A.R.) in this paper. The required amounts of $\text{Gd}(\text{NO}_3)_3 \cdot 6\text{H}_2\text{O}$, $\text{Ba}(\text{NO}_3)_2$, $\text{Fe}(\text{NO}_3)_3 \cdot 9\text{H}_2\text{O}$ and $\text{Ni}(\text{NO}_3)_2 \cdot 6\text{H}_2\text{O}$ were dissolved in deionized water under stirring and citric acid was added as the complexant with a molar ratio of citric acid:total metal cations = 1.8:1. The solution was converted to a viscous gel under heating and stirring conditions, and the gel was ignited to flame. The resultant ash-like material was calcined in air at 700 °C for 3 h, and then ball-milled in ethanol for 3 h, thus the black GBFN powders were obtained.

The BZCY powders with perovskite-type structure were prepared using $\text{Ba}(\text{NO}_3)_2$, $\text{ZrO}(\text{NO}_3)_2 \cdot 2\text{H}_2\text{O}$, $(\text{NH}_4)_2\text{Ce}(\text{NO}_3)_6$, $\text{Y}(\text{NO}_3)_3 \cdot 6\text{H}_2\text{O}$ and citric acid as starting materials. The pale-gray BZCY powders were obtained by calcining the ash-like material, resulted from a similar citric-nitrate process to the preparation of GBFN powders, at 1100 °C for 10 h.

2.2. Fabrication of the fuel cell with GBFN cathode

The obtained BZCY powders were blended with NiO and starch (as pore former) with a weight ratio of 35:65:10 through ball-milling in ethanol for 3 h. The well-mixed powders were pressed into a green pellet of 20 mm in diameter and 1 mm in thickness under 50 MPa, followed by pre-sintering at 1000 °C for 2 h as an anode substrate. Homogeneous and stable electrolyte (BZCY) slurry was prepared by mixing the BZCY powders with a homemade organic binder consisting of ethyl cellulose and terpineol. The weight ratio of BZCY powders to the organic binder was 0.6. The BZCY slurry was spin-coated onto the pre-sintered NiO-BZCY anode substrate. Three spin-coating cycles were needed to get an adequate thickness of BZCY electrolyte membrane. After dried for 30 min, the substrate-supported BZCY electrolyte membrane was sintered at 1400 °C for 8 h in air at a heating rate of 2 °C min⁻¹, the half cell was obtained. A part of the black GBFN powders obtained above were pressed into a pellet, calcined at 1000 °C for 8 h in air, and then ball-milled in ethanol for 3 h again. The as-prepared $\text{GdBaFeNiO}_{5+\delta}$ (GBFN) powders were mixed fully with a 10 wt.% ethyl cellulose-terpineol binder by ball-milling for 1 h to prepare the GBFN cathode slurry. Then, the slurry was screen-printed onto

the BZCY electrolyte membrane of the half cell, and co-sintered at 900 °C for 2 h in air to form a single cell.

2.3. Electrochemical measurements and characterization

The rest of the black GBFN powders obtained above were pressed into a pellet by a hydrostatic pressure of 200 MPa, and then sintered at 1000 °C for 8 h in air. The relative density, which was determined by the Archimedes technique, of the sintered GBFN sample was higher than 91% of theoretical density and used for electrochemical determinations. The fuel cell was tested from 600 to 700 °C with humidified hydrogen as fuel and humidified air as oxidant, respectively. The levels of humidification in hydrogen and air were all ~3 vol% H_2O . Fig. 1 shows schematically the electrochemical reactions and the transportation of protons through a dense proton-conducting ceramic membrane. The flow rate of the gases was 50 ml min⁻¹. The conductivity and the cell performance were determined by an electrochemical workstation (Zahner IM6ex). The applied frequency range was from 0.1 Hz to 100 kHz, and the signal amplitude was 20 mV.

The structures and phase purities of electrodes and electrolyte of the fuel cell were identified by powder X-ray diffraction (XRD) on a Panalytical X'pert Pro MPD diffractometer with Ni filter using Cu K_α radiation ($\lambda=0.15418$ nm) operating at 40 kV and 40 mA. The scanning range and rate were 20–80° and 2.00° min⁻¹, respectively. The microstructure of the fuel cell was observed by field-emission scanning electron microscopy (FESEM, Hitachi S-4700).

3. Results and discussion

It is clear from Fig. 2a that the GBFN cathode material sintered at 1000 °C for 8 h is a layered perovskite-type structure which is similar to that of the $\text{GdBaCo}_2\text{O}_{5+\delta}$ cathode reported by Tarancon et al. [17]. It is also clear from Fig. 2b that the BZCY membrane co-sintered at 1400 °C for 8 h is a well-crystallized single phase with perovskite-type structure. Fig. 2c displays the XRD pattern of anode substrate NiO-BZCY (weight ratio of 65:35) sintered at 1400 °C for 8 h. Obviously, the anode substrate only has the peaks corresponding well to BZCY as shown in Fig. 2b and NiO, and gives no evidence for the formation of other substance. In addition, the position of peaks of BZCY in Fig. 2(c) is almost the same as those in Fig. 2(b), indicating that little nickel was incorporated into the BZCY lattice [18].

It can be seen from the surface of BZCY electrolyte membrane sintered at 1400 °C for 8 h (Fig. 3a) that the electrolyte membrane is sufficiently dense, uniform and crack-free with an average grain size of 6–15 μm . It also can be seen from the cross-sectional image of the cell after tested (Fig. 3b) that the thickness of the electrolyte membrane is about 30 μm , and the membrane adheres to the anode substrate and the cathode firmly.

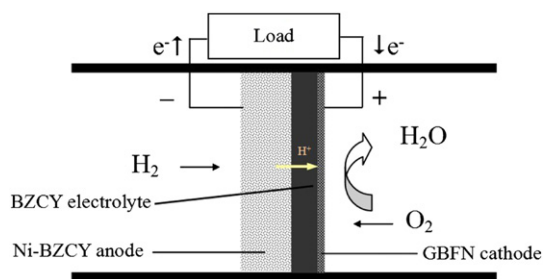


Fig. 1. Schematic of hydrogen transportation through a dense BZCY electrolyte membrane.

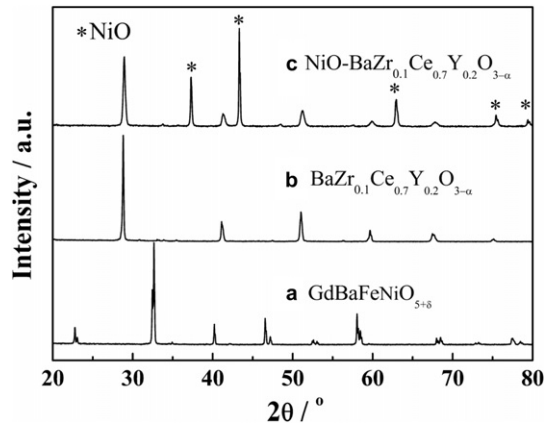


Fig. 2. XRD patterns for (a) GdBaFeNiO_{5+δ} (GBFN) cathode material sintered at 1000 °C for 8 h, (b) BZCY electrolyte membrane co-sintered at 1400 °C for 8 h, and (c) NiO–BZCY anode substrate sintered at 1400 °C for 8 h * marks peaks of NiO.

Fig. 4 shows the conductivities of the GBFN cathode material in the temperature range from 300 to 800 °C under oxygen, air and argon atmospheres. The conductivities are remarkably affected by the atmospheres and increase in the order: σ (in oxygen) > σ (in

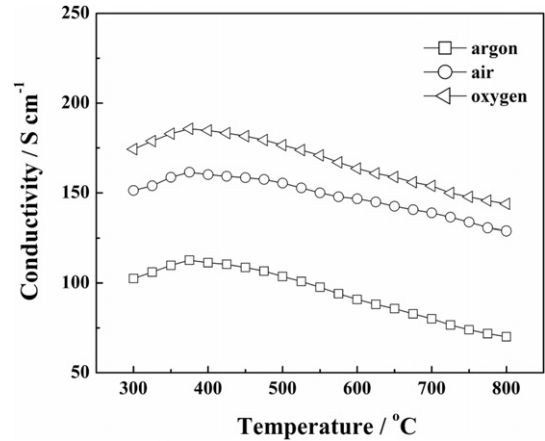


Fig. 4. Electrical conductivities of GBFN under argon, air and oxygen atmospheres.

air) > σ (in argon). This may be interpreted according to the following equation.



The equilibrium of the defect reaction shifts toward the right with oxygen partial pressure in the atmospheres increasing, thus resulting in an increase of electronic hole concentration and total conductivity of the GBFN cathode material.

The maximum conductivities are observed to be 112 S cm^{−1} under argon, 161 S cm^{−1} under air and 185 S cm^{−1} under oxygen, respectively. In addition, the GBFN reveals the trend, i.e. the conductivities first increase with increasing temperature up to 375 °C, and then decrease with further increasing temperature. The trend may be interpreted according to the following reason. The sample displays a semi-conductor conduction behavior between 300 and 375 °C, whereas a metallic-like conduction behavior above 375 °C. This trend is similar to that for SmBaCuFeO_{5+δ} [19], SmBaCuCoO_{5+δ} [19] and GdBaCo₂O_{5+δ} [17]. Nian et al. reported that the conductivities of SmBaCuFeO_{5+δ} and SmBaCuCoO_{5+δ} cathode materials reached 95–158 S cm^{−1} and 168–216 S cm^{−1} in air at 400–800 °C, respectively [19]. Tarancon et al. reported that the conductivities of GdBaCo₂O_{5+δ} cathode material reached 30–40 S cm^{−1} in air at 500–800 °C [17]. The conductivities of the GBFN cathode material reached 128–161 S cm^{−1} in air at 300–800 °C reported by us, which are comparable to those of SmBaCuFeO_{5+δ} [19] and lower than those of SmBaCuCoO_{5+δ} [19], but much higher than those of GdBaCo₂O_{5+δ} [17], indicating the GBFN has satisfactory conducting performance as cathode material for IT-SOFCs.

In the present study, the BZCY film exhibited a slightly higher conductivity of 0.014 S cm^{−1} than that (0.01 S cm^{−1}) of the pellet at 700 °C, possibly resulting from the same sintering temperature (1400 °C) and similar densification in the film and the pellet. In comparison, at the same temperature (700 °C), the conductivity (0.014 S cm^{−1}) of the BZCY film in this study is lower than (0.025 S cm^{−1}) of the BZCY film reported by Yang et al. [20] but in wet H₂ the conductivity (0.01 S cm^{−1}) of the pellet in this study is higher than that ($\sim 3.8 \times 10^{-3}$ S cm^{−1}) of the pellet reported by Yang et al. [20]. The differences in conductivity may be attributed to the different routes applied to prepare the BZCY films and the BZCY pellets.

The *I*–*V* and *I*–*P* performances of fuel cell based on the GBFN cathode are shown in Fig. 5. The open circuit voltages (OCVs) of the fuel cell are 1.05 V at 600 °C, 1.04 V at 650 °C and 1.02 V at 700 °C, respectively. The theoretical values of OCVs, which obtained from

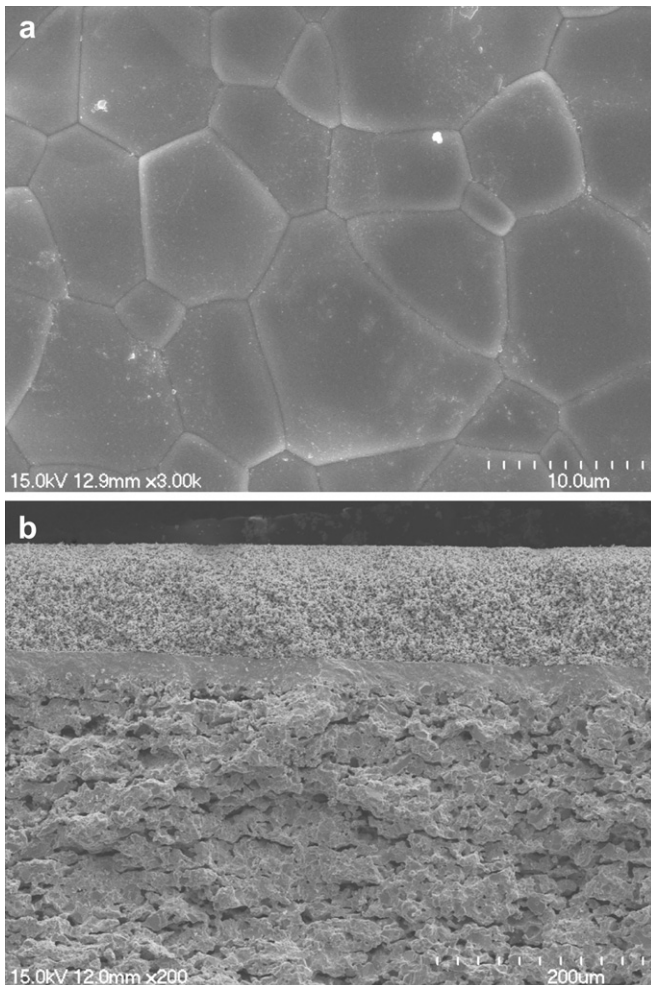


Fig. 3. Microstructures for (a) the surface of BZCY electrolyte membrane sintered at 1400 °C for 8 h and (b) the cross-section of the single cell after testing.

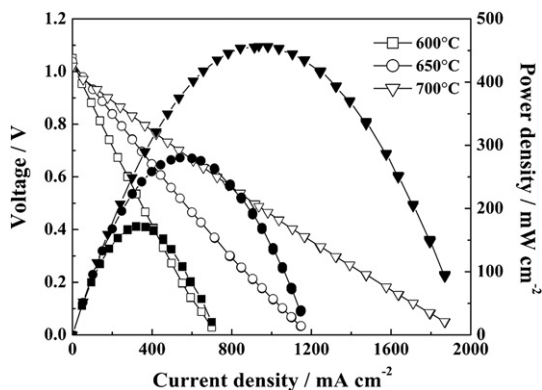


Fig. 5. I - V and I - P curves of fuel cell Ni-BZCY|BZCY|GBFN using hydrogen as the fuel and air as the oxidant at different temperatures.

equation (2), are 1.13 V at 600 °C, 1.12 V at 650 °C and 1.11 V at 700 °C, respectively. It is clear that the observed OCVs are close to the theoretical values, indicating the electrolyte membrane (thickness: 30 μm) is very dense. The maximum power densities of the fuel cell are 456 mW cm^{-2} at 700 °C, 280 mW cm^{-2} at 650 °C and 171 mW cm^{-2} at 600 °C, respectively. In spite of larger BZCY electrolyte membrane thickness, the power density is higher than that of the cell using a $\text{SmBaCo}_2\text{O}_{5+x}$ cathode and BZCY electrolyte with a thickness of 25 μm reported by Lin et al. [13]. Many SOFCs based on BZCY electrolyte and BZCY-LSCF, BZCY-SSC and SSC-SDC composite cathodes have been reported to display high fuel cell performances [20–23].

$$\text{EMF}_{\text{cal}} = \frac{RT}{4F} \left\{ \ln K - \left[P_{\text{H}_2\text{O(A)}} \cdot P_{\text{H}_2\text{O(C)}} / P_{\text{H}_2\text{(A)}}^2 \cdot P_{\text{O}_2\text{(C)}} \right] \right\} \quad (2)$$

In order to evaluate the performance of cathode (GBFN) in the fuel cell, the impedance spectra for the cell under open-current conditions at different temperatures are shown in Fig. 6. In the impedance spectra, the intercept with the real axis at low frequencies represents the total resistance of the cell (R_t) and the intercept at high frequency represents the ohmic resistance of the electrolyte (R_o). The difference between the R_o and R_t represents the interfacial polarization resistance of the cell (R_p), which contains the polarization resistances in cathode–electrolyte and anode–electrolyte interfaces. As shown in Fig. 6, the R_o and R_p are 0.79 $\Omega \text{ cm}^2$ and 0.77 $\Omega \text{ cm}^2$ at 600 °C, 0.57 $\Omega \text{ cm}^2$ and 0.32 $\Omega \text{ cm}^2$ at 650 °C, 0.42 $\Omega \text{ cm}^2$ and 0.15 $\Omega \text{ cm}^2$ at 700 °C, respectively. The R_p value of 0.15 $\Omega \text{ cm}^2$ in this paper is commensurate with that of 0.15 $\Omega \text{ cm}^2$ for the $\text{Ba}_{0.5}\text{Sr}_{0.5}\text{Fe}_{0.9}\text{Mo}_{0.1}\text{O}_{3-\delta}$ cathode reported by us [9] and lower than that of 0.18 $\Omega \text{ cm}^2$ for the $\text{GdBaFe}_2\text{O}_{5+\delta}$ cathode reported by Ding et al. [24] at 700 °C with same electrolyte and

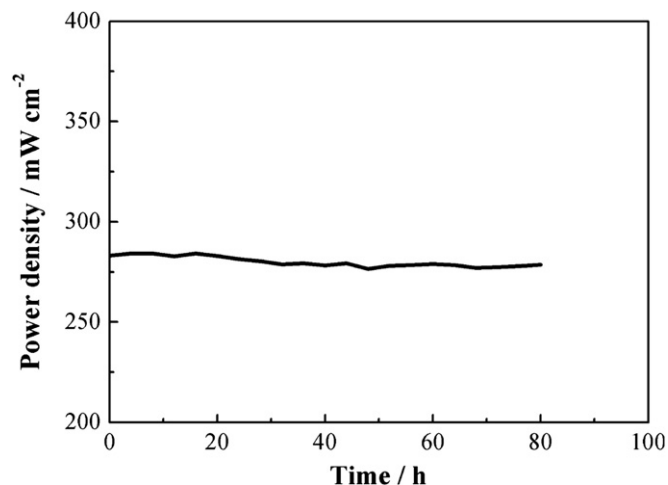


Fig. 7. The power output of the fuel cell as a function of operating time at 650 °C.

anode materials. Moreover, as shown in Fig. 7, no obvious degradation in the power output stability of the fuel cell was observed after operating at 650 °C for 80 h. However, the test of the power output stability over a longer period of time is in progress.

The satisfactory performance of IT-SOFC in this study is mainly attributed to the low interfacial polarization resistance of the fuel cell based on the GBFN cathode, indicating high electro-catalytic activity of the GBFN cathode for oxygen reduction. We compared the fuel cell performances with those reported in the literature for BZCY-based SOFCs. Yang et al reported the performances of the fuel cell based on anode-supported BZCY electrolyte films ($\sim 20 \mu\text{m}$ thick) from BZCY powders obtained from solid state reaction for the electrolyte and from a glycine nitrate process for the anode [20]. The peak power density reached $\sim 780 \text{ mW cm}^{-2}$ at 700 °C, which is higher than that of our fuel cell using anode-supported BZCY electrolyte film and GBFN cathode. This may be relevant to thicker BZCY film ($\sim 30 \mu\text{m}$ thick) and lower conductivity of the film as well as absence of cobalt (high catalytic activity on reduction of oxygen molecule) in the GBFN cathode. Sun et al. reported that the peak power density of the fuel cell using anode-supported BZCY electrolyte film ($\sim 30 \mu\text{m}$ thick) and Co-containing $\text{Sm}_{0.5}\text{Sr}_{0.5}\text{CoO}_{3-\delta}$ - $\text{Ce}_{0.8}\text{Sm}_{0.2}\text{O}_{2-\delta}$ composite cathode was $\sim 665 \text{ mW cm}^{-2}$ at 700 °C. In comparison with the fuel cells based on Co-containing composite cathodes, although the fuel cell performances in this study are lower, due to absence of expensive cobalt in the GBFN cathode, and also due to the favorable cell performances, the GBFN cathode is a promising candidate cathode material for proton-conducting IT-SOFCs.

4. Conclusions

In this study, a novel layered perovskite-type structure cathode material $\text{GdBaFeNiO}_{5+\delta}$ (GBFN) for proton conducting IT-SOFCs were prepared by a citric-nitrate process. The electrical conductivities of GBFN reached a maximum of 112 S cm^{-1} under argon, 161 S cm^{-1} under air and 185 S cm^{-1} under oxygen at 375 °C. The performance of the fuel cell Ni-BZCY|BZCY|GBFN was tested at 600–700 °C with hydrogen as the fuel and air as the oxidant. The OCVs of cell are close to the theoretical values, and the peak power densities reached 171 mW cm^{-2} at 600 °C, 280 mW cm^{-2} at 650 °C and 456 mW cm^{-2} at 700 °C, respectively. A low interfacial polarization resistance was observed to be 0.15 $\Omega \text{ cm}^2$ at 700 °C. The results indicate that the GBFN is a promising cobalt-free cathode material for proton-conducting IT-SOFCs.

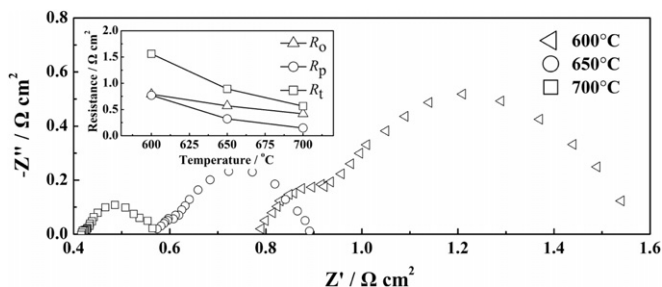


Fig. 6. Impedance spectra of the tested cell under open-current conditions at different temperatures. The inset shows the dependence of R_o , R_p and R_t of the cell on the temperature.

Acknowledgements

This work was supported by the National Natural Science Foundation of China (No. 20771079) and funded by the Priority Academic Program Development of Jiangsu Higher Education Institutions.

References

- [1] E.P. Murray, T. Tsai, S.A. Barnett, *Nature* 400 (1999) 649.
- [2] Z. Shao, S.M. Haile, *Nature* 431 (2004) 170.
- [3] W. Wang, Z. Yang, H. Wang, G. Ma, W. Gao, Z. Zhou, *J. Power Sources* 196 (2011) 3539.
- [4] W. Zhou, Z. Shao, R. Ran, P. Zeng, H. Gu, W. Jin, N. Xu, *J. Power Sources* 168 (2007) 330.
- [5] E. Wachsman, K. Lee, *Science* 334 (2011) 935.
- [6] K.H. Ryu, S.M. Haile, *Solid State Ionics* 125 (1999) 355.
- [7] C. Zuo, S. Zha, M. Liu, M. Hatano, M. Uchiyama, *Adv. Mater.* 18 (2006) 3318.
- [8] V. Dusastre, J.A. Kilner, *Solid State Ionics* 126 (1999) 163.
- [9] Z. Yang, W. Wang, J. Xiao, H. Zhang, F. Zhang, G. Ma, Z. Zhou, *J. Power Sources* 204 (2012) 89.
- [10] C. Huang, D. Chen, Y. Lin, R. Ran, Z. Shao, *J. Power Sources* 195 (2010) 5176.
- [11] A. Tarancon, S.J. Skinner, R.J. Chater, F. Hernandez-Ramirez, J.A. Kilner, *J. Mater. Chem.* 17 (2007) 3175.
- [12] S.H. Jo, P. Muralidharan, D.K. Kim, *Electrochem. Commun.* 11 (2009) 2085.
- [13] B. Lin, Y. Dong, R. Yan, S. Zhang, M. Hua, Y. Zhou, G. Meng, *J. Power Sources* 186 (2009) 446.
- [14] L. Zhao, B. He, Z. Xun, H. Wang, R. Peng, G. Meng, X. Liu, *Int. J. Hydrogen Energy* 35 (2010) 753.
- [15] G. Kim, S. Wang, A. Jacobson, L. Reimus, P. Brodersen, C. Mims, *J. Mater. Chem.* 17 (2007) 2500.
- [16] A.A. Taskin, A.N. Lavrov, Y. Ando, *Appl. Phys. Lett.* 86 (2005) 091910.
- [17] A. Tarancon, A. Morata, G. Dezanneau, S.J. Skinner, J.A. Kilner, S. Estrade, F. Ramirez, F. Peir, J. Morante, *J. Power Sources* 174 (2007) 255.
- [18] Z. Zhu, W. Sun, L. Yan, W. Liu, W. Liu, *Int. J. Hydrogen Energy* 36 (2011) 6337.
- [19] Q. Nian, L. Zhao, B. He, B. Lin, R. Peng, G. Meng, X. Liu, *J. Alloys Compd.* 492 (2010) 291.
- [20] L. Yang, C. Zuo, M. Liu, *J. Power Sources* 195 (2010) 1845.
- [21] L. Yang, C. Zuo, S. Wang, Z. Chen, M. Liu, *Adv. Mater.* 20 (2008) 3280.
- [22] L. Yang, Z. Liu, S. Wang, Y. Choi, C. Zuo, M. Liu, *J. Power Sources* 195 (2010) 471.
- [23] W. Sun, L. Yan, B. Lin, S. Zhang, W. Liu, *J. Power Sources* 195 (2010) 3155.
- [24] H. Ding, X. Xue, *J. Power Sources* 195 (2010) 4139.